Intelligent Monitoring Method of Aircraft Swashplate Plunger Pump Fluidity Based on Different Working Conditions

Chao Ma(✉) and Jinshou Shi

College of Aeronautical Engineering, Beijing Polytechnic, Beijing 100176, China
mczn05082023@163.com

Abstract. The swashplate plunger pump is one of the key components of the aircraft hydraulic transmission system, and its reliable operation is directly related to the flight safety of the aircraft. The key factor affecting the safety of swashplate plunger pumps is flowability. Therefore, an intelligent monitoring method for the flowability of aircraft swashplate plunger pumps based on different operating conditions is proposed. By analyzing the structure and working principle of the swashplate plunger pump, the types of abnormal flow phenomena are identified. Based on this, a multi-scale permutation entropy algorithm is used to extract the features of monitoring data. Due to the large amount of monitoring data features, fusion rules have been developed based on the feature fusion results of its traffic monitoring data. Based on the characteristics of abnormal flow data, an extreme learning machine is used to determine whether the flow of the swashplate plunger pump is abnormal, thereby achieving intelligent monitoring. The experimental data shows that under different experimental conditions, the flow monitoring results of the swash plate plunger pump obtained after the proposed method application are completely consistent with the actual results, with an accuracy of 100%; The monitoring time ranges from 0.20 s to 0.48 s, consistently not exceeding 0.5 s, and the monitoring efficiency is higher, fully confirming the better application performance of the proposed method.

Keywords: Aircraft Swashplate Plunger Pump · Intelligent Monitoring · Condition Monitoring · Mobility · Different Working Conditions

1 Introduction

The plunger pump is the key part of the whole hydraulic transmission system, and its main function is to provide enough hydraulic oil for the hydraulic system when the whole hydraulic system is working. At present, among the positive displacement pumps, only the plunger pump can achieve high pressure and high speed. With the development of hydraulic technology, the development trend of positive displacement hydraulic pump is gradually high-pressure. By comparing the characteristics of the axial pump and the radial pump, it can be concluded that the axial piston pump has the

L. Yun et al. (Eds.): ADHIP 2023, LNICST 549, pp. 251–267, 2024.
https://doi.org/10.1007/978-3-031-50549-2_18

advantages of compact structure, small unit power volume, long service life, high rated working pressure, light weight, convenient arrangement of variable mechanism, etc. [1]. Because of these advantages of plunger pump, the application of axial plunger pump is increasingly extensive. The disadvantages of axial piston pump are high manufacturing cost, more sensitive to oil pollution, and high requirements for oil filtering accuracy.

The axial piston pump can also be divided into two categories, the swashplate type and the inclined shaft type, which have their own characteristics in structure and advantages in practical application. The drive plate is used in the structure of the inclined shaft axial piston pump, which makes the plunger cylinder not bear lateral force during rotation. Therefore, the possibility of the cylinder block overturning the oil distribution plate is small, and it is also conducive to improving the working efficiency and stability of the plunger pair and the oil distribution part. In addition, the allowable inclination angle on the structure is large. However, the structure of the inclined shaft pump is relatively complex, which requires the use of large capacity thrust bearings. The poor workmanship limits its ability to work continuously under high-pressure environment, and the production cost is relatively high. The swashplate axial piston pump, compared with the swashplate axial piston pump, uses a hydrostatic support structure for two pairs of high-speed motion pairs - oil distribution plate and cylinder block, slipper and plunger, which eliminates the large capacity thrust bearing. The swashplate axial piston pump has the advantages of compact structure, good processability, low production cost, small volume and light weight. At present, swashplate axial piston pump has been widely used. The rated working pressure of swashplate axial piston pump is generally within the range of 21–35 MPa, the peak pressure is between 28–40 MPa, the rotating speed of the main shaft is generally below 3000 rpm, and the volume constant is mostly below 300–500 cm/rpm. In recent years, it has reached 2336 cm/rpm or even higher through development. Due to its own structure and performance requirements, the aircraft uses a swashplate axial piston pump.

For swashplate plunger pump, the main Failure cause are wear caused by long-term high load operation, fatigue cracks of key components, failure modes such as reduced efficiency, vibration noise caused by shoe loosening, and even direct stagnation. However, the aircraft Servomechanism adopts closed hydraulic oil circuit, with high motor speed, short single operation time and frequent start stop reversing [2]. Under this working condition, the plunger pump starts, stops, and reverses multiple times, causing sudden changes in internal pressure and causing impacts. The fault mode will mainly be cavitation caused by sudden changes in load and wear and leakage caused by friction pairs after multiple load impacts. The flowability of the swashplate plunger pump is the key factor affecting its normal operation, making it one of the urgent problems to design an effective intelligent monitoring method for the flowability of the aircraft swashplate plunger pump in the current aircraft field. In order to ensure the reliable operation of the swash plate plunger pump, researchers have proposed a method of monitoring the status of the plunger pump by extracting the oil temperature signal of the plunger pump to monitor power loss. But it will fail due to short single operation time, slow heat response, and fast heat loss. Researchers have also analyzed the iron filings content in hydraulic oil using ferrography to determine the wear of plunger pumps, but in practical applications, it is not suitable for plunger pumps installed in closed hydraulic oil circuits.

In addition, the use scenarios and equipment limitations of the aircraft Servomechanism also make the status monitoring of the plunger pump subject to many restrictions. For example, the acquisition of the vibration signal analysis spectrum will be difficult to extract features because of the excessive environmental noise of the Servomechanism, and the acquisition of the oil pressure signal to extract the pulse frequency analysis will be unable to extract the feature frequency band when the speed of the plunger pump is high due to the low sampling rate of the oil pressure sensor.

In response to the problems with the above methods, it is evident that there are significant differences in the effectiveness of state monitoring methods for general plunger pumps under different operating conditions. Therefore, in order to solve the above problems, this article proposes a research on intelligent monitoring method for the flowability of aircraft swashplate plunger pumps.

2 Research on the Intelligent Monitoring Method for the Fluidity of Swashplate Plunger Pump

2.1 Flow Analysis of Swashplate Plunger Pump

By analyzing the structure and working principle of swashplate plunger pump, the types of abnormal flow phenomena of swashplate plunger pump are clarified, which lays a solid foundation for the subsequent intelligent monitoring of swashplate plunger pump flow.

The piston at the hydraulic end of the swashplate plunger pump is driven by the crank connecting rod mechanism at the power end and reciprocates, thereby changing the pressure in the cylinder liner at the hydraulic end, opening and closing the suction valve and the discharge valve, thus realizing the basic function of medium transportation [3]. The structure of swashplate plunger pump is shown in Fig. 1.

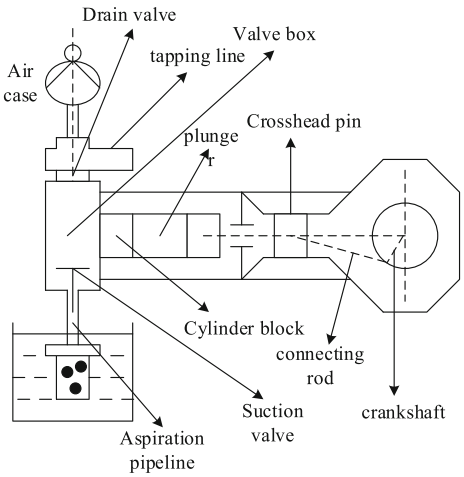

Fig. 1. Structure diagram of swashplate plunger pump

Taking the cylinder body of the pump head as an example, the working principle of its hydraulic end is explained. The crankshaft rotates to drive the plunger to reciprocate once, and the plunger pump executes the working cycle once, as shown in Fig. 2.

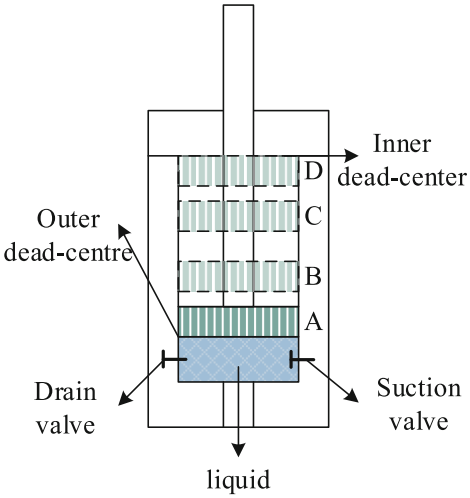

Fig. 2. Schematic diagram of working principle of swashplate plunger pump

As shown in Fig. 2, the working principle of the swashplate plunger pump is the four processes through which the closed volume liquid in the cylinder body passes, namely, expansion (A → B), liquid suction (B → C), compression (C → D), and liquid discharge (D → A), as shown below:

(1) Expansion (A → B)
When the piston is at A, the discharge valve of the pump head is in a critical closed state, but there is still some liquid left in the cylinder. When the plunger moves from the outer dead center to the inner dead center, the spring force makes the drain valve close, the sealed volume in the cylinder body gradually increases, and the vacuum degree in the space also gradually increases. When the force on one side of the suction valve pipeline is greater than the force in the pump, the suction valve opens. At this moment, the plunger moves to position B, and the liquid pressure in the cylinder body is also minimum.

(2) Sucking liquid (B → C)
After passing through point B, as the piston continues to move toward the inner dead center, the liquid flows into the cylinder block through the suction pipeline until it reaches the inner dead center C, and the volume of the cylinder block no longer increases.

(3) Compression (C → D)
When the crankshaft drives the piston to move outward from the inner dead center C, the spring acts on the liquid suction valve to close it, the liquid in the cylinder is compressed, the cylinder volume becomes smaller, and the liquid pressure increases;

When the plunger moves to D, the pressure in the cylinder is enough to push the drain valve open. At this moment, the liquid pressure is the maximum [4].

(4) Drain (D → A)
After passing through point D, as the piston continues to move outward to dead center A, the liquid continuously gushes out of the cylinder block through the discharge pipeline until it reaches the dead center, and the volume of the cylinder block no longer decreases. Then enter the next suction and discharge stroke.

It can be seen that the flow at the hydraulic end of the plunger pump is pulsating, and the liquid pressure in the pump changes periodically, and the liquid in the pipeline also belongs to the unstable flow state. The abnormal flow of swashplate plunger pump can be divided into several types, as shown in Table 1.

Table 1. Types of Abnormal Flow Phenomenon of Swashplate Plunger Pump

number	Trigger part	Principle causing abnormal liquidity
1	Pump valve assembly failure	Leakage of valve body, valve seat or valve rubber causes reduction of liquid discharge; The spring of the pump valve breaks and fails, causing serious delay in the closing of the pump valve, uneven discharge flow, and severe vibration
2	Wear of plunger and cylinder liner	The plunger or piston seal is damaged, the working medium leaks, and the liquid discharge is reduced; Plunger, cylinder liner or packing, resulting in increased clearance with cylinder liner, leakage of working medium, and reduced liquid discharge
3	Eccentric wear of plunger and cylinder liner	Due to the misalignment of the plunger or piston rod and crosshead pull rod, the eccentric wear between the plunger or piston and the cylinder liner is serious, and the surface of the cylinder liner rises significantly
4	Suction line/discharge line fault	The pipeline is not sealed tightly, and the circulating liquid leaks; The pipeline is blocked, and the pressure of pump controlled pumping or discharge pipeline increases significantly; Inadequate suction and reduced discharge due to improper installation of suction pipeline

It can be seen from Table 1 that the failure of multiple components in the swashplate plunger pump will lead to abnormal flow, which will affect the normal operation of the swashplate plunger pump. Therefore, intelligent monitoring of the swashplate plunger pump's flow has a vital role and significance.

2.2 Feature Extraction of Flow Monitoring Data of Swashplate Plunger Pump

In order to simplify the flow monitoring process of swashplate plunger pump, multi-scale permutation entropy algorithm is used to extract the characteristics of monitoring data, which provides a basis for subsequent monitoring information fusion.

Permutation entropy is a nonlinear processing method for signal analysis. Permutation entropy is an index to measure the complexity of time series, which is used to study the irregularity and chaos of nonlinear signals. Compared with Lyapunov exponent, sample entropy and other indicators, permutation entropy has the advantages of strong robustness, simple calculation and easy understanding [5]. In the fields of EEG signal, vibration signal and image processing, ideal research results have been achieved. Set the time series of swashplate plunger pump liquidity monitoring data as $\{x(i), i = 1, 2, \cdots, n\}$, and reconstruct the space to get a new time series, the form is as follows:

$$\begin{cases} X(1) = \{x(1), x(1+\alpha), \cdots, x(1+(m-1)\alpha)\} \\ \vdots \\ X(i) = \{x(i), x(i+\alpha), \cdots, x(i+(m-1)\alpha)\} \\ \vdots \\ X(n-(m-1)\alpha) = \{x(n-(m-1)\alpha), x(n-(m-2)\alpha), \cdots, x(n)\} \end{cases} \tag{1}$$

In formula (1), $\{X(i), i = 1, 2, \cdots, n-(m-1)\alpha\}$ represents a new time series; α represents the delay time; m it represents the embedded dimension.

Yes $\{X(i), i = 1, 2, \cdots, n-(m-1)\alpha\}$ arrange them in a gradually increasing order to obtain the corresponding symbol sequence. The expression is

$$\beta(g) = \{j_1, j_2, \cdots, j_m\} \tag{2}$$

In formula (2), $\beta(g)$ represents the symbol sequence corresponding to the new time series; j_m it refers to the no m symbols.

Then calculate the probability of occurrence of any one in all numbering sequences P_g, then the time series can be converted into $\{x(i), i = 1, 2, \cdots, n\}$ The permutation entropy of is defined as:

$$H(m) = -\sum_{g=1}^{k} P_g \ln P_g \tag{3}$$

In Eq. (3), $H(m)$ it represents the new definition of time series permutation entropy; k indicates the maximum number.

In order to facilitate the research, formula (3) is further processed and controlled between 0 and 1, which is expressed as

$$Y(i) = \frac{H(m)}{\ln(m!)} = \frac{-\sum_{g=1}^{k} P_g \ln P_g}{\ln(m!)} \tag{4}$$

In Eq. (4), $Y(i)$ it represents the final time series results of swashplate plunger pump liquidity monitoring data.

$Y(i)$ the size of shows the complexity and randomness of the time series. If $Y(i)$ a smaller value reflects a smaller change in the time series, while a larger value indicates a more complex time series. $Y(i)$ the change of can reflect the small change of a specific position in the time series and amplify it. Therefore, it is regarded as the characteristics of the flow monitoring data of swashplate plunger pump and recorded as $\{Y(i), i = 1, 2, \cdots, n\}$.

The selection of permutation entropy parameter is the key to the performance of feature extraction of swashplate plunger pump flow monitoring data. Therefore, it is necessary to determine the time delay and embedding dimension. Wherein, the delay time of phase space reconstruction α it should be large enough to ensure $x(i)$ and $x(i + \alpha)$ They are basically independent of each other, but they cannot be completely independent, because this will make them have no connection, so that they cannot reflect the dynamic characteristics of the system. Now, for the selection of delay time, there are two most common methods: autocorrelation function method and mutual information method [6]. The autocorrelation function only represents the linear correlation of two variables, while the cross-correlation function represents the overall correlation of two variables. A lot of research shows that the delay time determined by mutual information method α to be more suitable than the time delay determined by the autocorrelation function method, this paper also uses the mutual information method to determine the delay time. The mutual information of the two time series is expressed as:

$$I(\alpha) = \sum_{i=1}^{n} P[x(i), x(i+\alpha)] \log_2 \left[\frac{P[x(i), x(i+\alpha)]}{P[x(i)]P[x(i+\alpha)]} \right] \tag{5}$$

In formula (5), $I(\alpha)$ it means $x(i)$ and $x(i + \alpha)$ mutual information; $P[x(i)]$ it represents the probability of a single event in the first time series; $P[x(i + \alpha)]$ it represents the probability of a single event in the second time series; $P[x(i), x(i + \alpha)]$ it represents the joint probability of two events.

When $I(\alpha)$ equal to 0, the correlation between the two time series is also 0.In the phase space reconstruction process, select $I(\alpha)$ the time delay corresponding to the first minimum is taken as the time delay of phase space reconstruction.

For embedding dimension in phase space reconstruction m selection of, if m too small, the less time series will be obtained after phase space reconstruction, and the characteristics of the system cannot be well represented; If m the value of is too large, the analysis time will be too long, and the influence of interference signal will not be amplified. So embedding dimension m the selection of is equally important. In this study, the method of false adjacent points is selected to estimate the embedding dimension m

determine. When the embedding dimension is low, it may appear that the projection points of two points that were originally far away in the one-dimensional space are very close. These two points are called false proximity points. With the increase of embedding dimension, the distance between false neighboring points gradually increases. When the distance between false neighboring points is fully expanded, the embedding dimension is the minimum embedding dimension.

When the embedding dimension is m, the space points after phase space reconstruction of one-dimensional time series can be expressed as:

$$X(i) = \{x(i), x(i+\alpha), \cdots, x(i+(m-1)\alpha)\} \tag{6}$$

Set to space point $X(i)$, the adjacent space points are $X(j)$, then the Euclidean distance between the two adjacent points is:

$$d_m = \|X(i) - X(j)\|_2 = \sqrt{\sum_{k=1}^{m-1} \left[x(i+k\alpha) - x(j+k\alpha)\right]^2} \tag{7}$$

In Eq. (7), d_m means $X(i)$ and $X(j)$ the Euclidean distance between two adjacent points.

When the embedding dimension is $m+1$, the Euclidean distance between two space points is:

$$d_{m+1} = \|X(i) - X(j)\|_2 = \sqrt{\sum_{k=1}^{m} \left[x(i+k\alpha) - x(j+k\alpha)\right]^2} \tag{8}$$

When d_{m+1} than d_m if it is much larger, it indicates that these two space points are false adjacent points, that is, determine the minimum embedding dimension as d_m corresponding m value.

The determined time delay and embedding dimension are substituted into formula (1), and the final flow monitoring data characteristics of swashplate plunger pump can be obtained through formula (2), (3) and (4) $\{Y(i), i = 1, 2, \cdots, n\}$ to provide a basis for subsequent research.

2.3 Multi Sensor Monitoring Information Fusion

Multi sensor is used to monitor the flow of swashplate plunger pump. Due to the large amount of monitoring information, if it is directly applied, it will waste a lot of manpower and material resources, and reduce the calculation efficiency of the proposed method [7]. Therefore, this section carries out fusion processing for multi-sensor monitoring information.

Multi sensor monitoring information fusion refers to multi-level processing of multiple information. Each level of processing is the reprocessing and abstraction of the upper level information. According to its level in the fusion system, information fusion can be divided into three categories: data level fusion, feature level fusion and decision level fusion, as shown below:

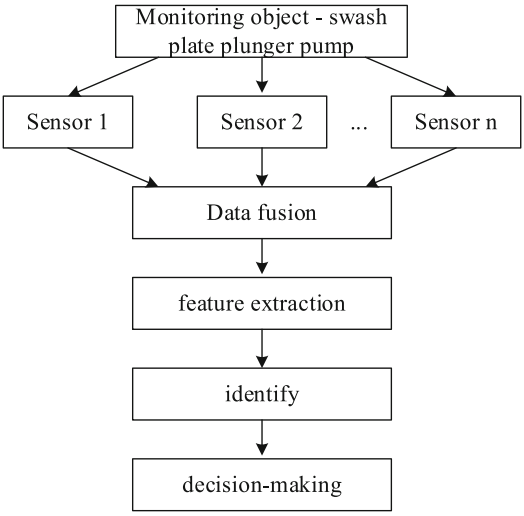

Fig. 3. Schematic diagram of data level fusion principle

First, data level fusion

The principle of data level fusion is shown in Fig. 3.

Data level fusion is the lowest level fusion, which is to directly fuse the data collected by sensors, that is, the data collected by sensors are comprehensively analyzed and processed without preprocessing, and then the subsequent feature extraction is performed from the fused information. Data set fusion requires that the sensors are of the same category, that is, the collected data are the same physical quantity or phenomenon. Data level fusion has less information loss and can provide subtle information, but it has large amount of information, time-consuming processing, large amount of communication and poor anti-interference ability.

Second, feature level fusion

The principle of feature level fusion is shown in Fig. 4.

Feature level fusion belongs to the middle layer. This method first extracts features from the original data collected by sensors, then fuses the feature data obtained by each sensor, and finally carries out the recognition and decision-making process. The method of feature level fusion is used to extract the features of the original information, which to some extent realizes the information compression and facilitates communication and real-time processing. At present, most of the practical application systems adopt the feature level fusion method [8].

Third, decision level integration

Decision level fusion is a high-level fusion. First, feature extraction, recognition and decision-making are carried out independently according to the original information of each sensor, and then the decision results are fused to get the final decision. Decision level fusion is the fusion of decision results. In theory, its effect is more accurate than that of a single sensor, but in practice, it needs to ensure that each sensor signal is independent,

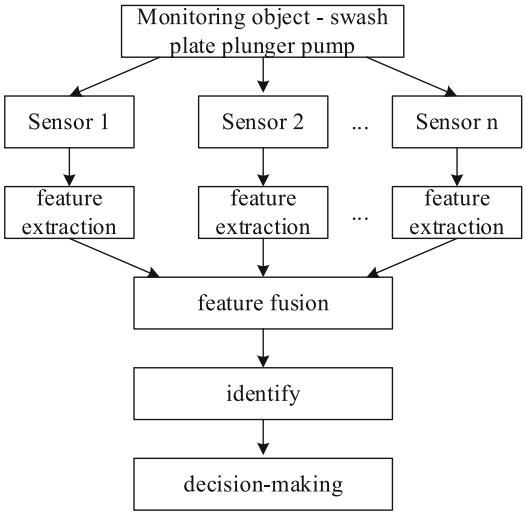

Fig. 4. Schematic diagram of feature level fusion principle

otherwise its performance may be lower than that of feature level fusion. Decision level fusion has small traffic, strong anti-interference ability and little dependence on sensors.

The principle of decision level fusion is shown in Fig. 5.

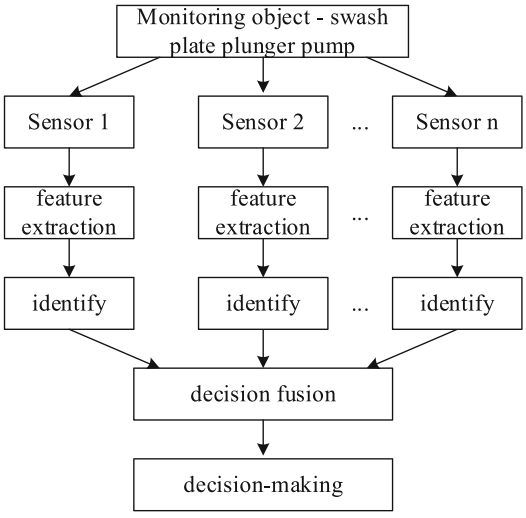

Fig. 5. Schematic Diagram of Decision Level Fusion Principle

Multi sensor information fusion technology can fuse different sensor data in different ways. When feature level fusion is adopted, recognition and decision-making are

required after feature fusion extracted from different sensors. This process requires mining potential data information and making decisions. Big data often hides more complex feature information, but the algorithm may not be able to fully learn these information, which will affect the performance of the model. Therefore, the feature information obtained from different algorithms or the feature information at different stages of the algorithm can be fused to form new fusion features, which will greatly improve the feature learning ability. This research proposes a feature fusion method, and the specific principle is shown in Fig. 6.

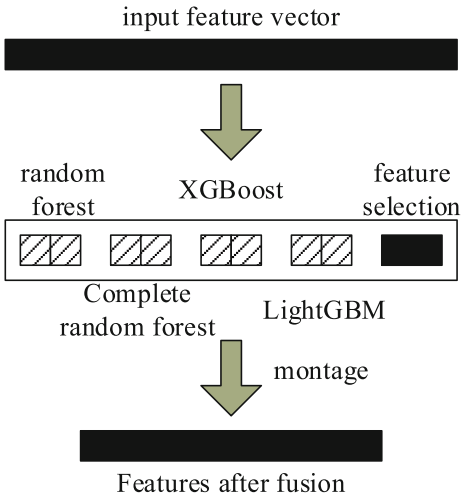

Fig. 6. Schematic diagram of feature fusion principle

As shown in Fig. 6, first train the integrated classifiers of random forest, completely random forest, XGBoost, LightGBM and so on using the original input features, and then train the class probability vector [9]. At the same time, the original input features are screened using random forests, or feature dimensionality is reduced through PCA and other methods to obtain the features after screening or feature dimensionality reduction; Finally, the category probability vector and the processed feature vector are spliced to obtain the final fusion feature. This feature fusion method can not only retain important feature information, but also take into account the global information, while removing redundant features and reducing feature dimensions. Then the fused features are trained using the deep forest model, which is the deep forest of multi feature fusion.

The above process completed the fusion of multi-sensor monitoring information, and obtained the swashplate plunger pump liquidity monitoring data feature fusion results as follows: $\{Z(i), i = 1, 2, \cdots, L\}$, L it represents the total number of fusion features, which facilitates the realization of intelligent monitoring of swashplate plunger pump fluidity.

2.4 Realization of Intelligent Monitoring of Swashplate Plunger Pump Fluidity

Feature fusion results of swashplate plunger pump flow monitoring data obtained above $\{Z(i), i = 1, 2, \cdots, L\}$ on the basis of, obtain the characteristics of liquidity anomaly data from existing literature $\{R(j), j = 1, 2, \cdots, W\}$ (W it indicates the total number of abnormal flow data characteristics), and the extreme learning machine (ELM) is used to determine whether the swashplate plunger pump has abnormal flow, so as to realize the intelligent monitoring of swashplate plunger pump flow and provide assistance for the stable operation of the plunger pump.

The network structure of the ELM model is the same as that of the single hidden layer feedforward neural network, but it is not the gradient based algorithm (backward propagation) in the traditional neural network in the training phase. Instead, the input layer weights and deviations are randomly assigned, and the output layer weights are calculated by the generalized inverse matrix theory. This structure can quickly complete the classification training of the flow state of the plunger pump while ensuring the accuracy. In practical application, only the weights and deviations on all network nodes need to be solved to complete the training of the limit learning machine model. When the characteristic parameters of the test set are input, the network output can be calculated through the weight of the output layer obtained to complete the determination of the piston pump's fluidity and achieve the purpose of liquidity monitoring [10].

Given training set $\{Z(i), T(i)\}$, $T(i)$ represents the i the flow state of the plunger pump at time units. The number of hidden layer nodes of the limit learning machine is N in this way, the network structure of the limit learning machine is established. Like the structure of the single hidden layer feedforward neural network, the input of the neural network from left to right is a training sample set, and there is a hidden layer in the middle [11]. From the input layer to the hidden layer, there is a full connection. Remember that the output of the hidden layer is $G(Z)$, then hide layer output $G(Z)$ the expression of is

$$G(Z) = \left[g_1(Z), g_2(Z), \cdots, g_N(Z)\right] \tag{9}$$

The output of the hidden layer is obtained by multiplying the input by the corresponding weight plus the deviation, and then summing all the node results of a nonlinear function. $G(Z) = \left[g_1(Z), g_2(Z), \cdots, g_N(Z)\right]$ is ELM nonlinear mapping (hidden layer output matrix), $g_k(Z)$ is the first k output of hidden layer nodes. The output functions of hidden layer nodes are not unique, and different output functions can be used for different hidden layer neurons [12]. In general, in practical applications, $g_k(Z)$ it is expressed as follows:

$$g_k(Z) = \zeta(\omega_k, \upsilon_k, Z) = \zeta(\omega_k Z + \upsilon_k) \tag{10}$$

In Eq. (10), $\zeta(\omega_k, \upsilon_k, Z)$ it represents the activation function and is a nonlinear piecewise continuous function satisfying the ELM general approximation ability theorem. Common activation functions include Sigmaid function, sine function, Hardlim function, etc. The activation function used in this modeling is Sigmaid function; ω_k and υ_k represents hidden layer node parameters.

Next, we deduce the transfer relationship from the hidden layer to the output layer. The output of the single hidden layer feedforward neural network ELM for "generalized" is:

$$f_N(Z) = \frac{\sum \psi_k g_k(Z)}{\xi(Z(i), R(j))} \tag{11}$$

In Eq. (11), $f_N(Z)$ it represents the judgment result of the flow state of swashplate plunger pump; ψ_k represents the output weight between the hidden layer and the output layer; $\xi(Z(i), R(j))$ it represents the correlation coefficient between the characteristics fusion result of swashplate plunger pump liquidity monitoring data and the characteristics of abnormal liquidity data [13].

According to the calculation results of formula (11), the piston pump liquidity monitoring rules are formulated as follows:

$$\begin{cases} f_N \leq \Psi^o \text{ Liquidity anomaly} \\ f_N > \Psi^o \text{ Normal liquidity} \end{cases} \tag{12}$$

In Eq. (12), Ψ^o it indicates the determination threshold value of the plunger pump liquidity state.

It should be noted that in the application process of the extreme learning machine, the establishment of the number of hidden layer nodes actually affects the accuracy of the model. The number of nodes is too much. Although the model can express more nonlinear characteristics, at the same time, the compatibility of model prediction is worse. When the data correlation between the test set and the training set is not strong enough, the prediction accuracy is very low; When the number of nodes is too small, the expression ability of nonlinear relationship is limited, that is, the model itself cannot accurately express the relationship of the training set, which will also reduce the prediction accuracy of the model. In practice, the number of nodes selected by default is roughly the same as the sample set size of the input layer, but in practice, the optimal number of nodes cannot be obtained from the algorithm optimization, and it is necessary to test the accuracy optimization of the model several times to finally obtain the optimal number of nodes.

Through the above process, the intelligent monitoring of the swashplate plunger pump's fluidity is completed, which helps the swashplate plunger pump to operate stably.

3 Experiment and Result Analysis

3.1 Establishment of Experimental Environment

In order to verify the application performance of the proposed method, an experimental environment is built, as shown in Fig. 7.

As shown in Fig. 7, the monitoring platform is equipped with a variety of sensors to collect flow related data during the operation of swashplate plunger pump, which meets the requirements of the proposed method application performance test.

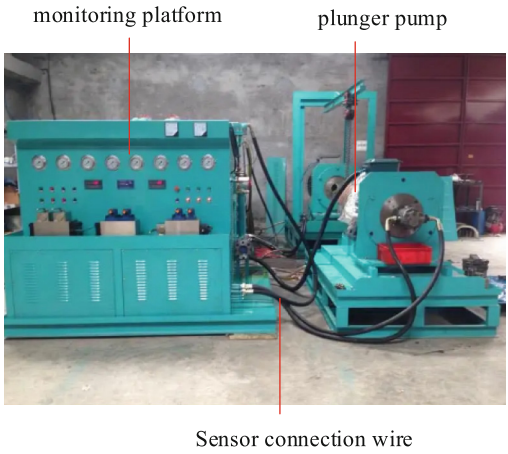

Fig. 7. Schematic Diagram of Experimental Environment

3.2 Setting of Test Conditions

The number of experimental conditions is also the key to affect the reliability of experimental conclusions. In order to improve the credibility of the experimental conclusions, this study has set up 10 different experimental conditions, as shown in Table 2.

Table 2. Setting table of test conditions

Test conditions	Monitoring data volume/MB	Liquidity status
1	4562	abnormal
2	3658	normal
3	4012	abnormal
4	4589	abnormal
5	3569	normal
6	5021	abnormal
7	4578	normal
8	3521	abnormal
9	2659	abnormal
10	3550	normal

As shown in Table 2, the monitoring data volume and liquidity status of the 10 experimental conditions are inconsistent, which indicates that the background conditions of each experimental condition are quite different and meet the requirements of the proposed method application performance test.

3.3 Analysis of Experimental Results

Based on the above built experimental environment and the set experimental conditions, and taking the condition monitoring method of the plunger pump based on the oil temperature signal and the condition monitoring method of the plunger pump based on the ferrography analysis method as the comparison methods 1 and 2, the flow monitoring comparison experiment of the swashplate plunger pump was carried out. In order to clearly show the application performance of the proposed method, the flow monitoring results and monitoring time of swashplate plunger pump are selected as evaluation indicators. The specific analysis process of experimental results is shown below.

The flow monitoring results of swashplate plunger pump obtained through experiments are shown in Table 3.

Table 3. Flow Monitoring Results of Swashplate Plunger Pump

Test conditions	Liquidity status	Propose method	Comparison method 1	Comparison method 2
1	abnormal	abnormal	abnormal	normal
2	normal	normal	abnormal	normal
3	abnormal	abnormal	normal	abnormal
4	abnormal	abnormal	abnormal	abnormal
5	normal	normal	normal	normal
6	abnormal	abnormal	abnormal	normal
7	normal	normal	normal	abnormal
8	abnormal	abnormal	abnormal	abnormal
9	abnormal	abnormal	normal	abnormal
10	normal	normal	normal	abnormal

As shown in Table 3, there are certain discrepancies between the flow monitoring results of the swash plate plunger pump obtained by comparison method 1 and the actual results. There are monitoring errors in three working conditions, with an accuracy rate of 70%; There are certain discrepancies between the flow monitoring results of the swash plate plunger pump obtained by comparison method 2 and the actual results, with monitoring errors occurring in 4 working conditions, with an accuracy rate of 60%; The flow monitoring results of the swashplate plunger pump obtained after the application of the proposed method are completely consistent with the actual results, with an accuracy of 100%; This indicates that the proposed method provides more accurate flow monitoring results for the swashplate plunger pump.

The flow monitoring time of swashplate plunger pump obtained through experiments is shown in Fig. 8.

As shown in the data in Fig. 8, the flow monitoring time of the swash plate plunger pump obtained by method 1 is 0.35 s–0.65 s, while the flow monitoring time of the swash

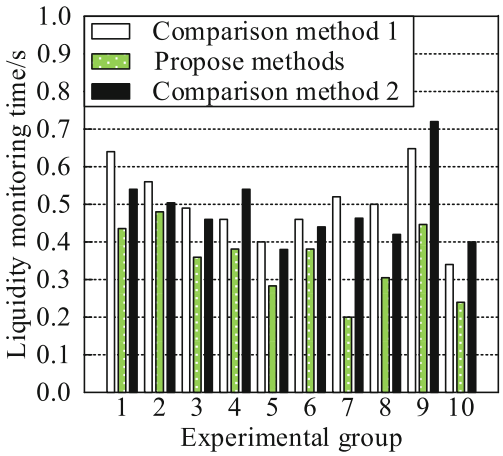

Fig. 8. Schematic diagram of flow monitoring time of swashplate plunger pump

plate plunger pump obtained by method 2 is 0.38 s–0.72 s. However, the flow monitoring time of the swash plate plunger pump obtained by method proposed after application is 0.20 s–0.48 s. The flow monitoring time of the swash plate plunger pump obtained by method proposed after application is lower than that of comparison methods 1 and 2, and always does not exceed 0.5s, this indicates that the proposed method has a higher efficiency in monitoring the flowability of the swashplate plunger pump.

4 Conclusion

The swashplate plunger pump is the key to the smooth flight of aircraft, and whether the swashplate plunger pump can operate stably depends on its own fluidity. Therefore, an intelligent monitoring method for the fluidity of aircraft swashplate plunger pumps based on different operating conditions is proposed. And through experiments, it was verified that the monitoring results of the proposed method are completely consistent with the actual results, with an accuracy of 100%; The monitoring time is 0.20 s to 0.48 s, always not exceeding 0.5 s, with higher monitoring efficiency, providing effective method support for the stable operation of the swashplate plunger pump and the aircraft. In our research, we will continue to improve our design methods, improve the real-time monitoring level of the swashplate plunger pump, and provide certain technical support for the smooth flight of the aircraft.

Acknowledgement. A school-level project of Beijing Polytechnic, Project Name: Research and application of the flowability of the aircraft swashplate plunger pump under different working conditions (2022X050-KXZ).

References

1. Liu, S., Chen, P., Woźniak, M.: Image enhancement-based detection with small infrared targets. Remote Sens. **14**, 3232 (2022)

2. Shao, N., Chen, Y.: Abnormal data detection and identification method of distribution internet of things monitoring terminal based on spatiotemporal correlation. Energies **15**(6), 2151 (2022)
3. Zhang, H., Ge, D., Yang, N., et al.: Study on internet of things architecture of substation online monitoring equipment. MATEC Web Conf. **336**(5), 05024 (2021)
4. Zhang, Y., Zou, X., Zhang, B., et al.: A flexible turning and sensing system for pressure ulcers prevention. Electronics **10**(23), 2971 (2021)
5. Liu, S., Lu, M., Liu, G.: A novel distance metric: generalized relative entropy. Entropy **19**(6), 269 (2017)
6. Santos, R., Leal-Junior, A.G., Ribeiro, M., et al.: Datacenter thermal monitoring without blind spots: FBG-based quasi-distributed sensing. IEEE Sens. J. **21**(8), 9869–9876 (2021)
7. Lim, Y.Y., Smith, S.T., Padilla, R.V., et al.: Monitoring of concrete curing using the electromechanical impedance technique: review and path forward. Struct. Health Monit. **20**(2), 604–636 (2021)
8. Liu, S., Wang, S., Liu, X., et al.: Human inertial thinking strategy: a novel fuzzy reasoning mechanism for IoT-assisted visual monitoring. IEEE Internet Things J. (2022). https://doi.org/10.1109/JIOT.2022.3142115
9. Li, H., Spencer, B.F., Liu, W., et al.: Multi-feature integration and machine learning for guided wave structural health monitoring: application to switch rail foot. Struct. Health Monit. **20**(4), 2013–2034 (2021)
10. Drouaz, M., Colicchio, B., Moukadem, A., et al.: New time-frequency transient features for nonintrusive load monitoring. Energies **14**(1437), 1437–1437 (2021)
11. Sun, Z., Wang, Y., Zhang, H., et al.: Parameter optimization and performance simulation evaluation of new swash plate-plunger energy recovery device. Desalin. Int. J. Sci. Technol. Desalt. Water Purif. **528**, 115598 (2022)
12. Pronyakin, V.I., Skrypka, V.L,, Abykanova, B.T.: Surface microgeometry monitoring of large-sized aircraft elements. IOP Conf. Ser. Mater. Sci. Eng. **1027**, 012024 (2021)
13. Saracyakupoglu, T.: A comprehensive fracture research of an aircraft swash-plate pump. Eng. Fail. Anal. **140** (2022)